Mechanical Forces Impacting Cleavage of Von Willebrand Factor in Laminar and Turbulent Blood Flow

Alireza Sharifi [1] and David Bark [2],*

[1] Department of Mechanical Engineering, Colorado State University, Fort Collins, CO 80523, USA; arsh@colostate.edu
[2] Department of Pediatrics, Washington University in Saint Louis, Saint Louis, MO 63130, USA
* Correspondence: bark@wustl.edu

Abstract: Von Willebrand factor (VWF) is a large multimeric hemostatic protein. VWF is critical in arresting platelets in regions of high shear stress found in blood circulation. Excessive cleavage of VWF that leads to reduced VWF multimer size in plasma can cause acquired von Willebrand syndrome, which is a bleeding disorder found in some heart valve diseases and in patients receiving mechanical circulatory support. It has been proposed that hemodynamics (blood flow) found in these environments ultimately leads to VWF cleavage. In the context of experiments reported in the literature, scission theory, developed for polymers, is applied here to provide insight into flow that can produce strong extensional forces on VWF that leads to domain unfolding and exposure of a cryptic site for cleavage through a metalloproteinase. Based on theoretical tensile forces, laminar flow only enables VWF cleavage when shear rate is large enough (>2800 s^{-1}) or when VWF is exposed to constant shear stress for nonphysiological exposure times (>20 min). Predicted forces increase in turbulence, increasing the chance for VWF cleavage. These findings can be used when designing blood-contacting medical devices by providing hemodynamic limits to these devices that can otherwise lead to acquired von Willebrand syndrome.

Keywords: von Willebrand factor; VWF; cleavage; shear; elongational flow; turbulence; acquired von Willebrand syndrome

1. Introduction

Hemostasis is the process where bleeding is stopped and in the event of vascular injury, the multimeric plasma protein von Willebrand Factor (VWF) mediates platelet adhesion and rolling through the glycoprotein (GP) Ibα of the GPIb-IX-V complex in regions of relatively high shear stress [1]. VWF is one of nature's longest proteins, up to 200 monomers for ultra-large VWF, with each monomer extending roughly 70 nm in length [1–3]. However, lower molecular weight VWF multimers are found in plasma under healthy conditions because ultra-large VWF from Weibel-Palade bodies in endothelial cells become exposed and cleaved at the A2 domain found on VWF at the endothelial cell surface by A Disintegrin and Metalloproteinase with Thrombospondin type 1 motif, member 13 (ADAMTS13). High molecular weight multimers in blood tend to have a size of roughly 5500–20,000 kDa, corresponding to 11–40 dimers, or 22–80 monomers. Cleavage is a critical step in maintaining normal hemostasis because hemostatic capacity increases with multimer size [4]. For example, lack of cleavage leads to thrombotic complications in thrombotic thrombocytopenic purpura [2]. Alternatively, mutations that lead to low molecular weight multimers results in a bleeding disorder known as von Willebrand disease [5]. VWF is also found in platelet α-granules, with a wide range of multimer sizes from dimers of 500 kDa to high molecular weight multimers and even ultra-large VWF. Overall, VWF from both endothelial cells and platelets can play an important role in hemostasis with the largest multimers contributing most to hemostasis.

VWF is highly force-sensitive, making it an intriguing protein from a mechanics perspective. It adopts a globular shape in normal circulation, where it is not very hemostatically active. Alternatively, when exposed to high shear stress or elongational flow, it has been demonstrated that VWF extends roughly $50\times$ from the globular form due to mechanical stress across the multimer [6]. It is believed that this extension increases the hemostatic function, whereas hemostatic capacity increases with the size of the VWF multimer, as mentioned. Increased function is likely related to a local threshold tension of roughly 21 pN, which unfolds the A1 domain, a subdomain of VWF that supports platelet GPIbα binding [7]. In laminar flow this is a two step process, initially involving VWF extension, followed by A1 domain unfolding. Comparatively and counteractively, A2 domain unfolding supports cleavage through ADAMTS13 via exposure of a cryptic site of the A2 domain and therefore reduces the hemostatic capacity. This process is critical in preventing VWF from triggering the formation of blood clots in normal circulation [8]. Excessive cleavage can lead to acquired von Willebrand syndrome (aVWS), a bleeding disorder seen in patients with mechanical circulatory support or some forms of heart valve disease, e.g., aortic stenosis [9,10]. The flow conditions in these patients (e.g., high shear stress and/or elongational flow), commonly described as pathologic, are proposed to cause the excessive VWF cleavage [11,12].

Mechanical forces in laminar and turbulent flow can cause VWF extension and cleavage. Multiple studies have assessed the effect of elongational flow and shear rate on VWF cleavage, with the latter consisting of both an extensional (principal stresses) and rotational component [13–18]. These studies demonstrated a globule-stretch transition near a shear rate of 5000 s^{-1}, as shear forces in the flow create tension on the polymer, or multimer in this case, and extends it [19]. However, more recent studies have demonstrated that turbulent flow conditions may significantly enhance VWF cleavage [20,21]. This could be due to increased mixing, collisions, high instantaneous shear stress, or through the interaction of turbulent eddies. To dissect out the processes leading to cleavage for turbulent flow, there remains a need to quantify the fluid forces relative to forces expected in laminar flow in relation to VWF cleavage.

Although given limited attention in VWF literature, polymer scission theories may provide insight in VWF cleavage seen in experiments. Polymer chains can be cleaved by mechanical forces in both laminar and turbulent flow with further modulation through the local chemical environment. The degradation of polymer chain primary bonds is called polymer chain scission in which the polymer chain breaks in one or several points along its backbone [22,23]. Polymer chains experience breakage in fluid flow due to the coupling of macroscale mechanical forces and microscale chemical processes. To link these disparate scales, a scaling theory for polymer scission has been introduced to relate fluid forces to the scission product distribution. The fluid force is typically quantified by the strain rate and the scission product distribution is quantified by the molar mass distribution of ruptured polymer chains [24,25]. Mechanically induced scission, such as the one caused by strong extensional flows, has been studied experimentally since at least the early seventies [26–28]. Scission theories for laminar and turbulent flow hypothesize that the drag force experienced by the chain creates sufficient tension to break the chain if the force is larger than the critical strength of a polymer covalent bond [29]. The assumption in laminar extensional flow is that the maximum tension is at the midpoint [30]. A threshold wall shear stress [31,32] or strain rate [33] is necessary to have a randomly coiled polymer extend prior to this breakage. This is the onset phenomenon. In predicting the onset phenomenon, researchers propose both length scale and time scale models. For the laminar flow, in the length scale model, the strain rate and polymer chain length affect the extensional force to initiate onset. In the time scale model, the onset occurs when the time ratio of polymer relaxation time to flow residence time (or Deborah number) is around unity. For the turbulent flow, onset occurs in the length scale model when the ratio of the polymer length scale to the turbulent length scale reaches a certain value. However, in the time scale model the onset occurs when the time ratio, which is the ratio of polymer relaxation time and the turbulent time, is around

unity. Both length and time scale models have been used to study the onset phenomena based on the polymer length, relaxation time, turbulent eddy size, and turbulent time scale. If the polymer size is several orders of magnitude smaller than the turbulent eddy size, the time scale model is typically used to compare the polymer relaxation time and the turbulent time scale [31–34]. Overall, the scission theories may at least provide insight into extensional forces existing along VWF, which may impact cleavage.

Because VWF is a multimer that has many similar features similar to a polymer, and because the mechanisms supporting VWF cleavage under fluid flow is not mechanistically fully characterized for laminar relative to turbulent flow, polymer scission theories are extended and utilized here to study VWF behavior in different flow regimes. This can improve our understanding of where and how VWF stretch can occur in relation to cleavage with a systematic mathematical approach. To do that, we have designed a study to investigate the VWF extension and breakage in different flow regimes by calculating the fluid forces that may work synergistically with ADAMTS13 to support cleavage. By identifying theoretical extensional forces for both laminar and turbulent flow, while relating them to cleavage seen in experiments, it is possible to assess what flow features mechanistically lead to acquired von Willebrand syndrome and to utilize the theory in both guiding surgical planning in the context of heart valve diseases and in the design of blood-contacting medical devices.

2. Method

In the current study, we are using the theoretical drag force in laminar and turbulent flow regimes to calculate the tensile force applied to VWF and to study its extension and breakage relative to reported experiments. It is noted that this is a theoretical study. The experimental data used in this study are taken from the literature listed in Table 1.

3. Laminar Flow

Based on a simple scaling theory for chain scission in laminar flow, the local fluid drag force is modeled with the following equation [29,35].

$$F_d \sim \chi \mu R^2 \tag{1}$$

μ is solvent viscosity, χ is principal strain rates and R is the polymer length scale, which is a function of the Deborah number (De). De is defined as the ratio of polymer (or multimer) relaxation time to flow residence time, and therefore defines how stretched VWF is likely to be. The residence time is the period that the polymers experience a specific strain rate, listed in Table 1. The time taken by the polymer to return from the deformed state to its initial equilibrium state is called the relaxation time which is on the order of 100 ms for VWF [36,37].

When De << 1, chains are assumed fully stretched and R is defined as the VWF contour length. Contour length is the length at maximum possible extension, which is equal to the product of the number of monomers with their length. R exhibits a large range that depends on multimer size from ~70 nm to 150 microns [4,7,38]. We note that ultra-large VWF multimers should not exist in plasma, except in pathological conditions. Alternatively, when De >> 1, chains adopt a globular-like conformation where R is approximated by the radius of gyration, estimated at 50–150 nm for VWF [39,40]. Because R is smaller for De >> 1 compared to De << 1, the force is also inherently smaller.

Note that the impact of VWF rotation on the predicted force is neglected in the current study, but it could impact upon the effective exposure time used to define the Deborah number because VWF in shear would experience cycling tension and compression along a specific axis, as opposed to sustained tension.

4. Turbulent Flow

In turbulent flow, the tensile drag force is conceptually set by the turbulent energy cascade [29],

$$F_d \sim \gamma \mu R^2 \tag{2}$$

where γ is the strain rate of velocity fluctuations associated with a specific spatial length scale (r), μ is the dynamic viscosity of the solvent, and R is the polymer length. γ is characterized based on 3 different categories. In the analysis, it is assumed that velocity fluctuations are on the order of the mean velocity, the largest eddy length scale is in the order of the characteristic length scale, and the Kolmogorov length scale is $\eta \sim dRe^{-3/4}$ [41]. The characteristic length is the dimension that defines the length scale of a physical flow, e.g., diameter of a vessel, or gap size in a rheometer [20]. By using the Taylor microscale formula ($r \sim \left(\frac{10\nu k}{\varepsilon} \right)^{1/2}$), we can approximate γ. At the largest length scale, the strain rate is given by

$$\gamma \sim \frac{\mu Re_L}{\rho L^2},\tag{3}$$

where Re_L is Reynolds number, which is based on the characteristic length scale of the flow, ρ is the density, and L is the characteristic length scale. In the inertial subrange ($\eta < r < L$),

$$\gamma \sim \frac{\mu Re_L}{\rho L^2} \left(\frac{r}{L} \right)^{-2/3},\tag{4}$$

where the strain rate increases as r decreases toward η which is the Kolmogorov length scale where energy is theoretically dissipated by viscosity. Once r decreases to the Kolmogorov length scale, the velocity gradient is assumed to be homogeneous and

$$\gamma \sim \frac{\mu Re_L^{3/2}}{\rho L^2}.\tag{5}$$

5. Result and Discussion

Table 1 shows the previous studies focused on VWF extension or cleavage in experiments from the literature. Data provided in the table parameterizes calculations for Equations (1)–(5) and is used to compare experimental VWF elongation and/or cleavage to predictions of theoretical force.

Table 1. Parameters found in experimental studies where, NM: Not measured, N/A: Not applicable, χ: principal strain rate, γ: turbulent flow strain rate, η: Kolmogorov length scale, t_e: exposure time.

Case	Flow Regime	γ, χ (1/s)	η (µm)	t_e (s)	Extended	Unfolded	Cleaved	Ref.
1	Laminar	200–3000	N/A	0.2–0.5	NM	NM	No	[20,21]
2	Laminar	4000–5000	N/A	NM	Yes	Yes	No	[42]
3	Laminar	10,000	N/A	1200–8400	NM	NM	Yes	[42]
4	Laminar	5000–10,000	N/A	0.1–0.3	Yes	Yes	NM	[11]
5	Laminar	200–130,000	N/A	0.001–0.1	NM	NM	No	[21]
6	Turbulent	2000–6000	10–40	0.0002–0.001	NM	NM	Yes	[20]
7	Turbulent	5000–10,000	20–35	0.0001–0.001	NM	NM	Yes	[21]
8	Turbulent	300,000	NM	10	NM	NM	Yes	[43]

Drag force from Equation (1) for laminar flow is compared to VWF cleavage from the literature, Table 1. Note that multimer size can vary substantially in a blood sample, from 500 kDa for a dimer with an estimated contour length of ~140 nm to >10,000 kDa for high molecular weight multimers found in plasma, corresponding to a contour length of >2.8 µm. However, the impact of VWF cleavage on hemostatic capacity occurs with the loss of high molecular weight multimers (>~1.5 µm), which is the focus of the current assessment. With this range, the applied extensional force in laminar flow escalates with increasing contour length for De << 1 which is shown in Figure 1, as flow residence time exceeds polymer relaxation time (~0.1 s). To unfold the A2 domain, 10–22 pN [44–47] of tension must exist locally across the domain, which is expected to occur near the multimer center. In addition, the average lifetime of VWF and ADAMTS13 bonds is maximized at 22 pN [48]. For high 5500–10,000 kDa multimers, cleavage is expected when shear rates exceed 10,000 s^{-1}, but could theoretically commence at shear rates greater than physiological values of 2800 s^{-1}. Increasing the contour length to 15 µm, requires a lower strain rate of 100 s^{-1} for optimized

A2 unfolding. Therefore, the largest multimers experience the highest tensile force across A2, while cleavage to a smaller size leads to less chance for additional cleavage of less hemostatically active VWF multimers. These results do not preclude cleavage at lower shear rates because rupture/cleavage can still occur at lower tensile forces (<20 pN) if enough time is given, just with less probability [45]. Overall, the combination of exposure time, shear rate, and multimer size leads to cleavage, as in agreement with Lippok et al. [42].
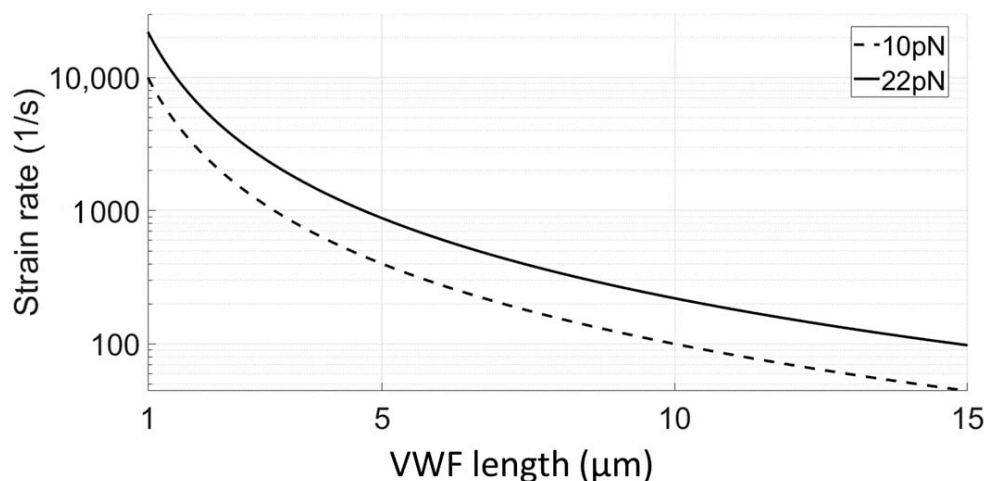

Figure 1. Force applied to VWF in laminar flow for a Deborah number much smaller than 1.

Compared to De << 1, De >> 1 exhibits much lower drag force values, as shown in Figure 2 for a large range of strain rates. The maximum drag force for De >> 1 is larger than the critical force to extend VWF, and is far beyond the critical force for A2 domain unfolding. VWF in Case 5 (Table 1) experience a drag force larger than 0.4 pN, which is enough force for VWF extension. Based on these results, extension, or cleavage of VWF is unlikely when flow for De >> 1, which means that VWF would require long flow exposure times to decrease De so that sufficient tension is experienced for VWF extension, which would be required to achieve sufficient forces for deficient cleavage, which is in agreement with the literature that demonstrates the need for a 2 step process of extension followed by cleavage [7].

Turbulent flow is also considered because laminar flow requires both very high shear rates, Figure 1, and very long (nonphysiological) exposure times [42]. Based on experimental studies demonstrating cleavage in turbulent flow in Table 1 [20,21], the spatial inertia scale (r) is in the range of 100 to 900 μm. The Kolmogorov length scale (η) is in the range of 3 to 40 μm. The drag forces when the spatial scale is equal to the characteristic length scale are shown in Figure 3a. The drag force is not large enough to cause unfolding or cleavage of VWF. Drag forces for the turbulent inertial range ($\eta < r < d$) are shown in Figure 3b. The drag force increases with VWF contour length, similar to laminar flow. However, for a given contour length, it is much higher in turbulent flow, with the largest molecular weight multimers receiving the highest tensile force. When the spatial length scale gets close to the smallest value of 100 μm, the drag force is the largest, meaning that the smallest eddies have the largest impact on VWF extension and domain unfolding. Conceptually, interactions between the smallest eddies would create large local transient forces, while large eddies entrain VWF without the large fluctuations seen at the smaller scales. A region of 10–22 pN is highlighted in the figure to show a threshold of where cleavage is expected. As the inertial scale decreases down to the Kolmogorov length scale, the drag force becomes very large, Figure 3c. High molecular weight multimers (>1.5 μm) have a high probability for cleavage at this scale based on the force magnitude, which is in agreement with the literature, Table 1 [21]. Energy from turbulence at this scale would be absorbed by viscosity, as well as protein and cell deformation. We hypothesize that in the inertial and Kolmogorov length scales, VWF cleavage does not require a two-step

process of (1) extension and (2) domain unfolding. Instead, intriguingly, a concentration of high intermittent stress could occur at many points around VWF in a globular state, as opposed to a single point at the center of extended VWF in suspension, making cleavage much more efficient [44]. Comparatively, even for shear rates of 5000 s^{-1}, substantial loss of high molecular weight multimers is seen in experiments within minutes for turbulent flow, compared to a time scale of hours for laminar flow [20,42]. It is noted that the analysis does not account for intermittency and shear stress fluctuations, which can otherwise significantly enhance instantaneous tensile forces [49]. In conclusion, a large Reynolds number (Re_L), leading to turbulence could increase the probability for the loss of high molecular weight VWF multimers. Furthermore, higher Re_L leads to smaller scale turbulent structure, which should lead to increased extensional force, as shown in Figure 3.
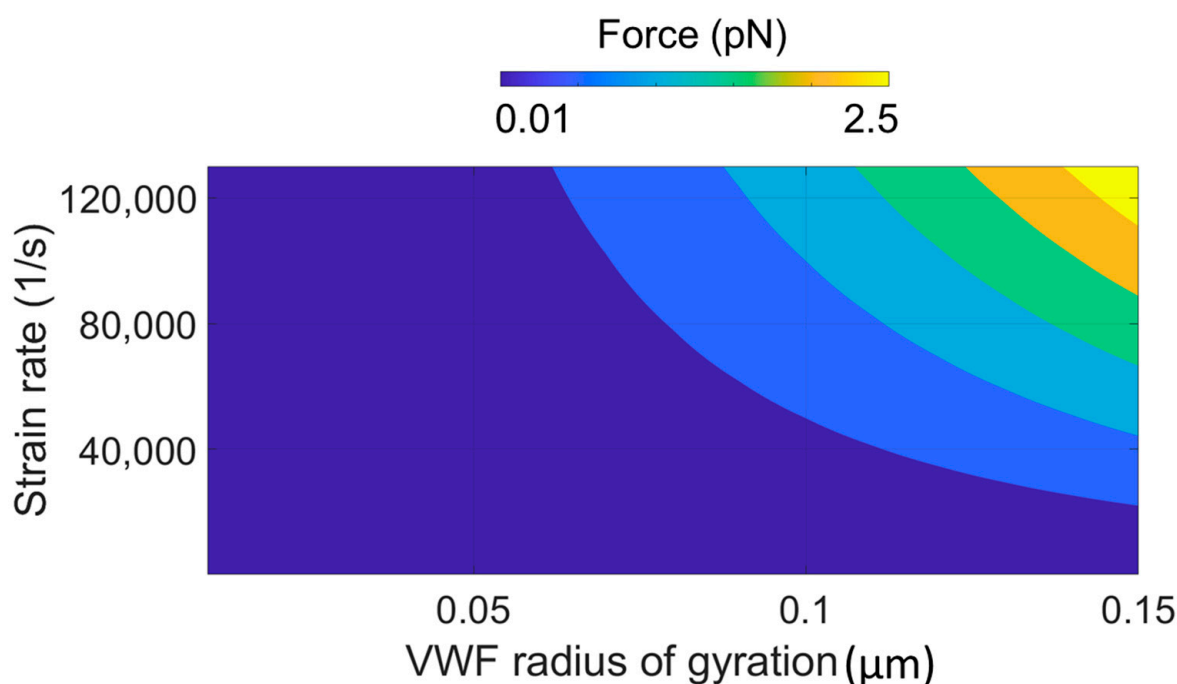

Figure 2. Force applied to VWF in laminar flow when the Deborah Number is much larger than 1.

An overall summary of the findings is presented in Figure 4. VWF extension, where De << 1, is required to obtain sufficient forces for domain unfolding and cleavage in laminar flow. However, laminar flow is inefficient at cleaving high molecular weight multimers because it cleaves at a single region in the center of an extended multimer, where tension is highest, after sustained exposure [42]. The highest molecular weight multimers experience the highest tensile forces, thereby exposing the largest region (largest number of adjacent monomers) where A2 unfolding is expected, while smaller multimers may not have efficient cleavage due to lower expected forces. Without high shear or nonphysiological exposure times, cleavage is not likely in laminar flow [19,20] This extreme condition is possible in laminar flow by using cone-and-plate viscometer [11]. However, the exposure time needs to be large enough to cause VWF cleavage which is not physiological. The exposure time in the body is the fraction of a second for the shear rates >5000 s^{-1} [21]. Alternatively, for turbulent flow, interacting eddies might lead to cleavage at multiple sites, while VWF remains in a globular form, regardless of the local shear rate, which is in agreement with experiments [19]. In turbulent flow, primary parameters that can influence VWF A2 unfolding include the Reynolds number and multimer size. As the Reynolds number increases, there is an increased amount of turbulent structures, with smaller scale structures. The current work demonstrates that the smallest scale turbulent structures have the biggest effect on tensile forces within VWF, which can become much higher than the forces found for laminar flow. Overall, turbulent flow is expected to lead to

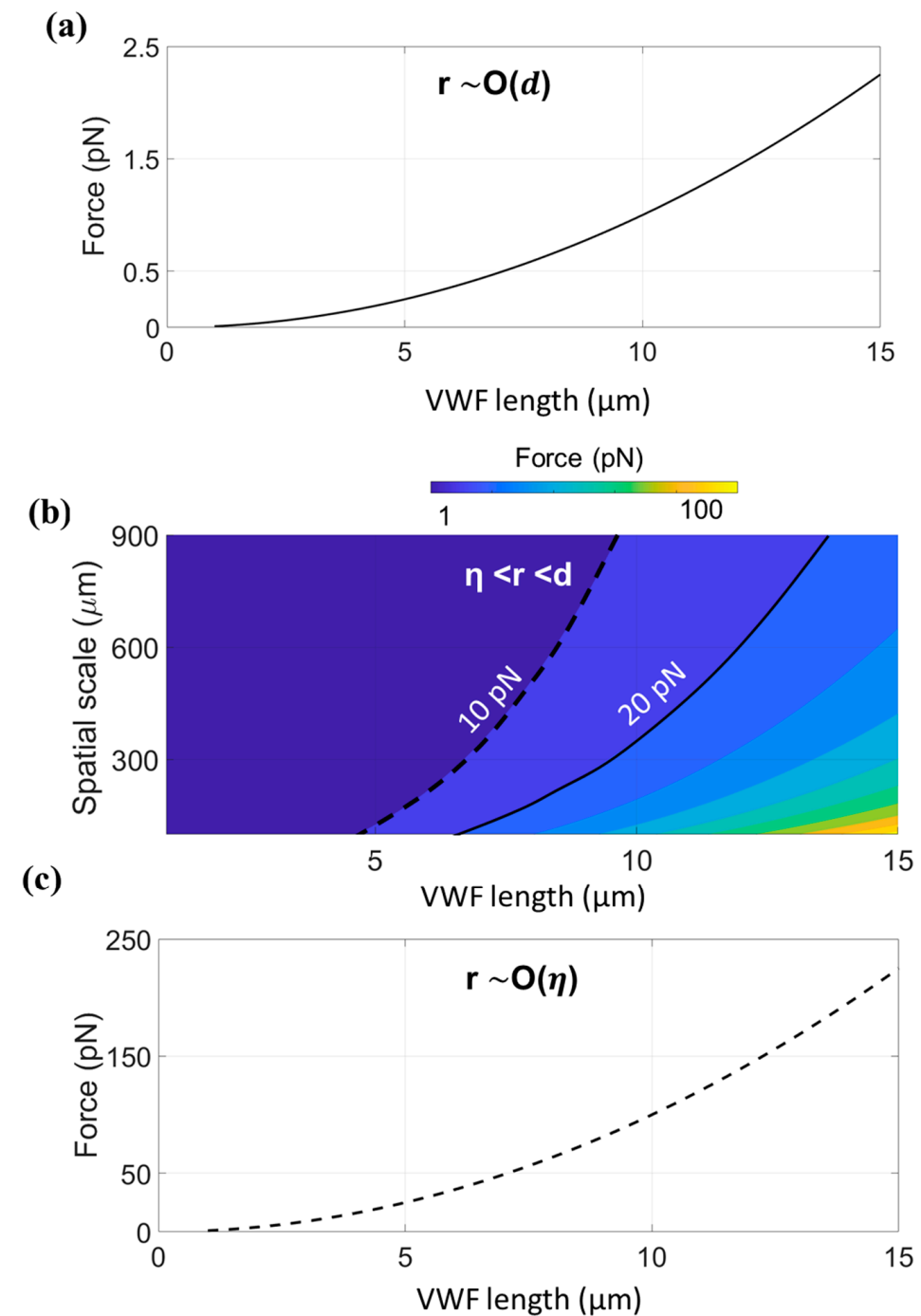efficient cleavage of VWF when compared to laminar flow due to high spatially disperse extensional forces.

Figure 3. Force applied to VWF in the turbulent flow for different VWF contour length and spatial scale of (**a**) largest length scale $r \sim O(d)$, (**b**) the inertial range ($\eta < r < d$), the critical force for unfolding is in the range of 10–22 pN (**c**) the smallest length scale $r \sim O(\eta)$.
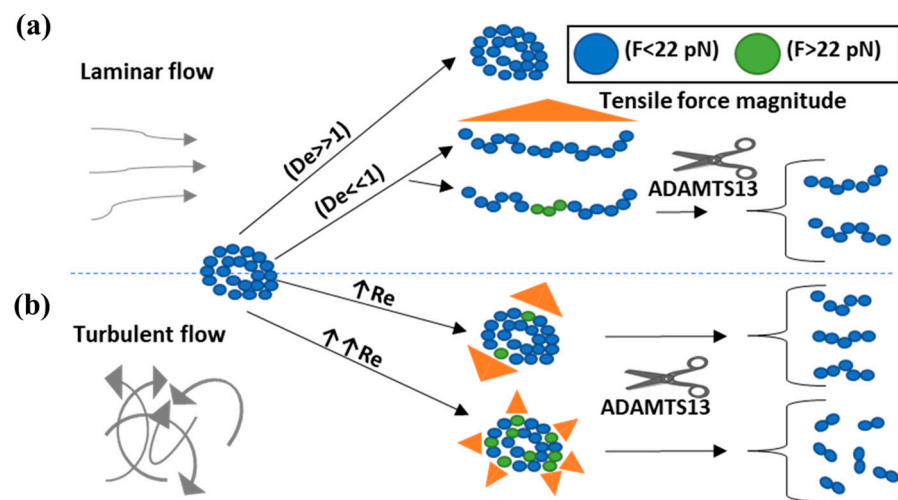
Figure 4. Hypothetical drawing of the VWF stretch and cleavage in (**a**) laminar flow (**b**) turbulent flow.

There are several assumptions in the current study. The calculated drag force is an approximation for both the laminar and turbulent flow. For laminar flow, the exact tensile force would depend on the instantaneous orientation of VWF relative to principal stresses, would depend on rotation, and specific shapes or conformations. In calculated the De number, the exposure time is highly simplified, whereas VWF extension likely depends on the type of flow, i.e., shear vs. elongational flow. This is because rotation of VWF in flow typical of shear flow would cycle VWF through compressive and tensile states, whereas elongational flow would create sustained tensile forces along a single direction. A scaling theory for Deborah numbers on the order of 1 becomes complex because polymers for a sufficiently large strain rate exist in a transitional state between globular and extended configurations as the relaxation time approaches the characteristic period of the flow. Such trends are seen in experiments, but are difficult to characterize with simple analytical approaches [50]. Therefore, only the limiting Deborah numbers (De << 1 or De >> 1) are presented to demonstrate drag force limits that likely exist in specific laminar flow environments. For turbulent flow, the actual tensile force and distribution of tensile forces along a VWF multimer remains theoretical. The theories used in this study do not account for effects from a solid wall. We assume homogeneous and isotropic turbulence. There is no calculation for the transitional flow regime that might exist in some of the cited experiments. Lastly, polymer scission theories are being applied to biological multimers, which can otherwise experience different behaviors, such as self-association.

6. Conclusions

Scission theory, developed for polymers, has been applied to study theoretical forces that could exist across the A2 domain of VWF in a suspension of fluid. Calculations combined with experimental observations from the literature demonstrate how several flow parameters can have an impact upon VWF cleavage. In laminar flow, either nonrealistic exposure times are needed to see cleavage based on the theory. However, in the turbulent flow, large tensile forces are expected in VWF, regardless of prior extension. These tensile forces are primarily dominated by small turbulent structures near or at the Kolmogorov scale.

Author Contributions: Both authors contributed equally to this article. Conceptualization, A.S. and D.B.; methodology, A.S. and D.B.; formal analysis, A.S. and D.B.; writing—original draft preparation, A.S. and D.B.; writing—review and editing, A.S. and D.B. All authors have read and agreed to the published version of the manuscript.

Data Availability Statement: The data presented in this study are available on request from the corresponding author.

Conflicts of Interest: The authors declare no conflict of interest.

References

1. Savage, B.; Saldívar, E.; Ruggeri, Z.M. Initiation of Platelet Adhesion by Arrest onto Fibrinogen or Translocation on von Willebrand Factor. *Cell* **1996**, *84*, 289–297. [CrossRef]
2. Sadler, J.E. New Concepts in von Willebrand Disease. *Annu. Rev. Med.* **2005**, *56*, 173–191. [CrossRef]
3. Savage, B.; Almus-Jacobs, F.; Ruggeri, Z.M. Specific Synergy of Multiple Substrate–Receptor Interactions in Platelet Thrombus Formation under Flow. *Cell* **1998**, *94*, 657–666. [CrossRef]
4. Stockschlaeder, M.; Schneppenheim, R.; Budde, U. Update on von Willebrand Factor Multimers: Focus on High-Molecular-Weight Multimers and Their Role in Hemostasis. *Blood Coagul. Fibrinolysis* **2014**, *25*, 206–216. [CrossRef] [PubMed]
5. Bharati, K.P.; Prashanth, U.R. Von Willebrand Disease: An Overview. *Indian J. Pharm. Sci.* **2011**, *73*, 7–16. [CrossRef] [PubMed]
6. Sadler, J.E. Biochemistry and Genetics of von Willebrand Factor. *Ann. Rev. Biochem* **1998**, *67*, 395–424. [CrossRef] [PubMed]
7. Springer, T.A. Von Willebrand Factor, Jedi Knight of the Bloodstream. *Blood J. Am. Soc. Hematol.* **2014**, *124*, 1412–1425. [CrossRef]
8. Zheng, X.L. ADAMTS13 and von Willebrand Factor in Thrombotic Thrombocytopenic Purpura. *Annu. Rev. Med.* **2015**, *66*, 211–225. [CrossRef]
9. Geisen, U.; Brehm, K.; Trummer, G.; Berchtold-Herz, M.; Heilmann, C.; Beyersdorf, F.; Schelling, J.; Schlagenhauf, A.; Zieger, B. Platelet Secretion Defects and Acquired von Willebrand Syndrome in Patients with Ventricular Assist Devices. *J. Am. Heart Assoc.* **2018**, *7*, e006519. [CrossRef]
10. Vincentelli, A.; Susen, S.; Le Tourneau, T.; Six, I.; Fabre, O.; Juthier, F.; Bauters, A.; Decoene, C.; Goudemand, J.; Prat, A. Acquired von Willebrand Syndrome in Aortic Stenosis. *N. Engl. J. Med.* **2003**, *349*, 343–349. [CrossRef]
11. Schneider, S.W.; Nuschele, S.; Wixforth, A.; Gorzelanny, C.; Alexander-Katz, A.; Netz, R.R.; Schneider, M.F. Shear-Induced Unfolding Triggers Adhesion of von Willebrand Factor Fibers. *Proc. Natl. Acad. Sci. USA* **2007**, *104*, 7899–7903. [CrossRef] [PubMed]
12. Sing, C.E.; Alexander-Katz, A. Elongational Flow Induces the Unfolding of von Willebrand Factor at Physiological Flow Rates. *Biophys. J.* **2010**, *98*, L35–L37. [CrossRef] [PubMed]
13. Doyle, P.S.; Shaqfeh, E.S. Dynamic Simulation of Freely-Draining, Flexible Bead-Rod Chains: Start-up of Extensional and Shear Flow. *J. Non-Newton. Fluid Mech.* **1998**, *76*, 43–78. [CrossRef]
14. Alexander-Katz, A.; Netz, R.R. Dynamics and Instabilities of Collapsed Polymers in Shear Flow. *Macromolecules* **2008**, *41*, 3363–3374. [CrossRef]
15. Sunthar, P.; Nguyen, D.A.; Dubbelboer, R.; Prakash, J.R.; Sridhar, T. Measurement and Prediction of the Elongational Stress Growth in a Dilute Solution of DNA Molecules. *Macromolecules* **2005**, *38*, 10200–10209. [CrossRef]
16. Neelov, I.M.; Adolf, D.B.; Lyulin, A.V.; Davies, G.R. Brownian Dynamics Simulation of Linear Polymers under Elongational Flow: Bead–Rod Model with Hydrodynamic Interactions. *J. Chem. Phys.* **2002**, *117*, 4030–4041. [CrossRef]
17. Venkataramani, V.; Sureshkumar, R.; Khomami, B. Coarse-Grained Modeling of Macromolecular Solutions Using a Configuration-Based Approach. *J. Rheol.* **2008**, *52*, 1143–1177. [CrossRef]
18. Harrison, G.M.; Remmelgas, J.; Leal, L.G. The Dynamics of Ultradilute Polymer Solutions in Transient Flow: Comparison of Dumbbell-Based Theory and Experiment. *J. Rheol.* **1998**, *42*, 1039–1058. [CrossRef]
19. Alexander-Katz, A.; Schneider, M.F.; Schneider, S.W.; Wixforth, A.; Netz, R.R. Shear-Flow-Induced Unfolding of Polymeric Globules. *Phys. Rev. Lett.* **2006**, *97*, 138101. [CrossRef]
20. Bortot, M.; Ashworth, K.; Sharifi, A.; Walker, F.; Crawford, N.C.; Neeves, K.B.; Bark, D., Jr.; Di Paola, J. Turbulent Flow Promotes Cleavage of VWF (von Willebrand Factor) by ADAMTS13 (a Disintegrin and Metalloproteinase with a Thrombospondin Type-1 Motif, Member 13). *Arterioscler. Thromb. Vasc. Biol.* **2019**, *39*, 1831–1842. [CrossRef]
21. Bortot, M.; Sharifi, A.; Ashworth, K.; Walker, F.; Cox, A.; Ruegg, K.; Clendenen, N.; Neeves, K.B.; Bark, D.; Di Paola, J. Pathologic Shear and Elongation Rates Do Not Cause Cleavage of Von Willebrand Factor by ADAMTS13 in a Purified System. *Cell. Mol. Bioeng.* **2020**, *13*, 379–390. [CrossRef] [PubMed]
22. McNaught, A.D.; Wilkinson, A. *Compendium of Chemical Terminology*; Blackwell Science Oxford: Oxford, UK, 1997; Volume 1669.
23. Koltzenburg, S.; Maskos, M.; Nuyken, O. *Polymere: Synthese, Eigenschaften Und Anwendungen*; Springer: Berlin/Heidelberg, Germany, 2013.
24. Frenkel, J. Orientation and Rupture of Linear Macromolecules in Dilute Solutions under the Influence of Viscous Flow. *Acta Phys. URSS* **1944**, *19*, 51–76.
25. Vanapalli, S.A.; Ceccio, S.L.; Solomon, M.J. Universal Scaling for Polymer Chain Scission in Turbulence. *Proc. Natl. Acad. Sci. USA* **2006**, *103*, 16660–16665. [CrossRef]
26. Horn, A.F.; Merrill, E.W. Midpoint Scission of Macromolecules in Dilute Solution in Turbulent Flow. *Nature* **1984**, *312*, 140–141. [CrossRef]
27. Keller, A.; Odell, J.A. The Extensibility of Macromolecules in Solution; A New Focus for Macromolecular Science. *Colloid Polym. Sci.* **1985**, *263*, 181–201. [CrossRef]
28. Nguyen, T.Q.; Kausch, H.-H. Chain Scission in Transient Extensional Flow Kinetics and Molecular Weight Dependence. *J. Non-Newton. Fluid Mech.* **1988**, *30*, 125–140. [CrossRef]

29. Universal Scaling for Polymer Chain Scission in Turbulence, PNAS. Available online: https://www.pnas.org/content/103/45/16660.short (accessed on 23 November 2020).
30. Perkins, T.T.; Smith, D.E.; Chu, S. Single Polymer Dynamics in an Elongational Flow. *Science* **1997**, *276*, 2016–2021. [CrossRef] [PubMed]
31. Drag Reduction Fundamentals—Virk—1975—AIChE Journal. Wiley Online Library. Available online: https://aiche.onlinelibrary.wiley.com/doi/abs/10.1002/aic.690210402?casa_token=URnE3nKXNBkAAAAA:eSiXageo-olThvJFFEA_cy_Jr-nJKekdnKjiS6SXX7suJtIQSOXv-fT-oQllup_O2WTbgwLrI5AdMcY (accessed on 23 November 2020).
32. Gold, P.I.; Amar, P.K.; Swaidan, B.E. Friction Reduction Degradation in Dilute Poly(Ethylene Oxide) Solutions. *J. Appl. Polym. Sci.* **1973**, *17*, 333–350. [CrossRef]
33. Hershey, H.C.; Zakin, J.L. A Molecular Approach to Predicting the Onset of Drag Reduction in the Turbulent Flow of Dilute Polymer Solutions. *Chem. Eng. Sci.* **1967**, *22*, 1847–1857. [CrossRef]
34. Virk, P.S.; Merrill, E.W. The Onset of Dilute Polymer Solution Phenomena. In *Viscous Drag Reduction*; Wells, C.S., Ed.; Springer: Boston, MA, USA, 1969; pp. 107–130.
35. Odell, J.A.; Keller, A. Flow-Induced Chain Fracture of Isolated Linear Macromolecules in Solution. *J. Polym. Sci. Part B Polym. Phys.* **1986**, *24*, 1889–1916. [CrossRef]
36. Steppich, D.M.; Angerer, J.I.; Sritharan, K.; Schneider, S.W.; Thalhammer, S.; Wixforth, A.; Alexander-Katz, A.; Schneider, M.F. Relaxation of Ultralarge VWF Bundles in a Microfluidic–AFM Hybrid Reactor. *Biochem. Biophys. Res. Commun.* **2008**, *369*, 507–512. [CrossRef] [PubMed]
37. Fu, H.; Jiang, Y.; Yang, D.; Scheiflinger, F.; Wong, W.P.; Springer, T.A. Flow-Induced Elongation of von Willebrand Factor Precedes Tension-Dependent Activation. *Nat. Commun.* **2017**, *8*, 324. [CrossRef] [PubMed]
38. Fowler, W.E.; Fretto, L.J.; Hamilton, K.K.; Erickson, H.P.; McKee, P.A. Substructure of Human von Willebrand Factor. *J. Clin. Investig.* **1985**, *76*, 1491–1500. [CrossRef] [PubMed]
39. Singh, I.; Shankaran, H.; Beauharnois, M.E.; Xiao, Z.; Alexandridis, P.; Neelamegham, S. Solution Structure of Human von Willebrand Factor Studied Using Small Angle Neutron Scattering. *J. Biol. Chem.* **2006**, *281*, 38266–38275. [CrossRef] [PubMed]
40. Slayter, H.; Loscalzo, J.; Bockenstedt, P.; Handin, R.I. Native Conformation of Human von Willebrand Protein. Analysis by Electron Microscopy and Quasi-Elastic Light Scattering. *J. Biol. Chem.* **1985**, *260*, 8559–8563. [CrossRef]
41. Pope, S.B. Turbulent Flows. *Meas. Sci. Technol.* **2001**, *12*, 2020. [CrossRef]
42. Lippok, S.; Radtke, M.; Obser, T.; Kleemeier, L.; Schneppenheim, R.; Budde, U.; Netz, R.R.; Rädler, J.O. Shear-Induced Unfolding and Enzymatic Cleavage of Full-Length VWF Multimers. *Biophys. J.* **2016**, *110*, 545–554. [CrossRef]
43. Jhun, C.-S.; Reibson, J.D.; Cysyk, J.P. Effective Ventricular Unloading by Left Ventricular Assist Device Varies with Stage of Heart Failure: Cardiac Simulator Study. *Asaio J.* **2011**, *57*, 407–413. [CrossRef]
44. Morabito, M.; Dong, C.; Wei, W.; Cheng, X.; Zhang, X.F.; Oztekin, A.; Webb, E. Internal Tensile Force and A2 Domain Unfolding of von Willebrand Factor Multimers in Shear Flow. *Biophys. J.* **2018**, *115*, 1860–1871. [CrossRef]
45. Wu, T.; Lin, J.; Cruz, M.A.; Dong, J.; Zhu, C. Force-Induced Cleavage of Single VWFA1A2A3 Tridomains by ADAMTS-13. *Blood* **2010**, *115*, 370–378. [CrossRef]
46. Ying, J.; Ling, Y.; Westfield, L.A.; Sadler, J.E.; Shao, J.-Y. Unfolding the A2 Domain of Von Willebrand Factor with the Optical Trap. *Biophys. J.* **2010**, *98*, 1685–1693. [CrossRef] [PubMed]
47. Zhang, X.; Halvorsen, K.; Zhang, C.-Z.; Wong, W.P.; Springer, T.A. Mechanoenzymatic Cleavage of the Ultralarge Vascular Protein von Willebrand Factor. *Science* **2009**, *324*, 1330–1334. [CrossRef] [PubMed]
48. Li, Z.; Lin, J.; Sulchek, T.; Cruz, M.A.; Wu, J.; Dong, J.; Zhu, C. Domain-Specific Mechanical Modulation of VWF–ADAMTS13 Interaction. *MBoC* **2019**, *30*, 1920–1929. [CrossRef] [PubMed]
49. Morshed, K.N.; Bark, D., Jr.; Forleo, M.; Dasi, L.P. Theory to Predict Shear Stress on Cells in Turbulent Blood Flow. *PLoS ONE* **2014**, *9*, e105357. [CrossRef]
50. Schroeder, C.M. Single Polymer Dynamics for Molecular Rheology. *J. Rheol.* **2018**, *62*, 371–403. [CrossRef]